Received: 11 April 2023 | Accepted: 6 May 2023

DOI: 10.1002/mma.9417

RESEARCH ARTICLE

WILEY

A generalization of the Kelvin–Voigt model with pressure-dependent moduli in which both stress and strain appear linearly

Hiromichi Itou[1] | **Victor A. Kovtunenko**[2,3] | **Kumbakonam R. Rajagopal**[4]

[1]Department of Mathematics, Tokyo University of Science, Tokyo, Japan

[2]Institute for Mathematics and Scientific Computing, University of Graz, NAWI Graz, Graz, Austria

[3]Lavrentyev Institute of Hydrodynamics, Siberian Division of the Russian Academy of Sciences, Novosibirsk, Russia

[4]Department of Mechanical Engineering, Texas A&M University, College Station, Texas, USA

Correspondence
Victor A. Kovtunenko, Institute for Mathematics and Scientific Computing, University of Graz, NAWI Graz, Heinrichstr. 36, 8010 Graz, Austria.
Email: victor.kovtunenko@uni-graz.at

Communicated by: M. Efendiev

Funding information
Japan Society for the Promotion of Science (JSPS), Grant/Award Number: 18K03380; Austrian Science Fund (FWF); Office of Naval Research; National Science Foundation; University of Graz

A generalization of the Kelvin–Voigt model that can represent viscoelastic materials whose moduli depend on the mechanical pressure is derived from an implicit constitutive relation in which both the Cauchy stress and the linearized strain appear linearly. For consistency with the assumption of small deformation, a thresholding approach is applied. The proposed mixed variational problem is investigated for its well-posedness within the context of maximal monotone and coercive graphs. For isotropic extension or compression, a semi-analytic solution of the generalization of the Kelvin–Voigt problem under stress control is presented. The corresponding numerical simulation for monotone and cyclic pressure loading is carried out, and the results then compared against the linearized model.

KEYWORDS

creep, cyclic behavior, implicit constitutive response, Kelvin–Voigt material, maximal monotone graph, mixed variational problem, nonlinear parabolic system, thresholding, viscoelasticity

MSC CLASSIFICATION

35Q74, 49J52, 74D10

1 | INTRODUCTION

Implicit constitutive relations for both fluids and solids have been studied in a systematic manner. The implicit constitutive relation introduced by Rajagopal [1]:

$$f(\mathbf{F}, \dot{\mathbf{F}}, \mathbf{T}, \dot{\mathbf{T}}) = 0 \tag{1}$$

is a special sub-class of the implicit functional constitutive relations between the history of the stress $\mathbf{T}$, the history of the density, and the history of the deformation gradient $\mathbf{F}$ (see Průša and Rajagopal [2]). The constitutive relation (1) represents the response of a class of viscoelastic bodies. A further sub-class of (1) wherein

$$f(\mathbf{F}, \mathbf{T}) = 0$$

represents the response relation of elastic bodies.

Recently, a particular sub-class of (1) was introduced by Rajagopal [3] and Rajagopal and Wineman [4] in which both the Cauchy stress $\mathbf{T}$ and the linearized strain $\boldsymbol{\varepsilon} \approx (\mathbf{F}^{\top}\mathbf{F}-\mathbf{I})/2$ appear linearly. Such material response is not linear as it contains the mutual product of stress and strain, but its special structure allows one to have linearly inhomogeneous material moduli. Well-posedness for the corresponding variational problems was established in Itou et al. [5, 6] by thresholding the moduli, if they can become unbounded.

Thomson [7] and Voigt [8] independently developed the viscoelastic solid constitutive relation that now bears their name, which is a sub-class of the constitutive relation (1). Boltzmann [9] was the first to develop a linear integral constitutive relation for the response of viscoelastic bodies. Many models to describe the viscoelastic response of solids using multiple integral constitutive relations, rate type constitutive relations, and differential type constitutive relations have been developed since this early works of Kelvin [7], Voigt [8], and Boltzmann [9] (see, e.g., Green and Rivlin [10, 11], Green et al. [12], Lockett [13], Muliana et al. [14], and Rajagopal and Srinivasa [15]). Implicit constitutive relations for viscoelasticity, from the view point of mathematical analysis, were carried out by Bulíček et al. [16, 17] and Itou et al. [18, 19] within the context of strain-limiting models, and in Itou et al. [20, 21] quasi-linear models were used to study the Boussinesq problem. The reader will find the treatment of nonlinear and unilateral boundary conditions used in viscoelastic problems in previous studies [22–26].

We shall consider the following generalization of a compressible Kelvin–Voigt material undergoing small deformation such that both the strain $\boldsymbol{\varepsilon}$ and the time rate of strain $\dot{\boldsymbol{\varepsilon}}$ are small:

$$\alpha_1(1+\lambda_1\mathrm{tr}\mathbf{T})\boldsymbol{\varepsilon}+\alpha_2(1+\lambda_2\mathrm{tr}\mathbf{T})\dot{\boldsymbol{\varepsilon}}=\mathbf{T}+(\alpha_3\mathrm{tr}\boldsymbol{\varepsilon}+\alpha_4\mathrm{tr}\dot{\boldsymbol{\varepsilon}})\mathbf{I}, \tag{2}$$

where $\mathbf{I}$ is the identity transformation, and six moduli $\alpha_1, \dots, \alpha_4, \lambda_1, \lambda_2$ are constants. The constitutive relation (2) includes as special cases linearized elastic and compressible linearized Kelvin–Voigt constitutive relations. The constitutive relation (2) is not a linear constitutive relation since terms involving products of variables $\boldsymbol{\varepsilon}$ or $\dot{\boldsymbol{\varepsilon}}$ and $\mathbf{T}$ appear, though they appear linearly. We note that $\mathrm{tr}\mathbf{T}$ is the mechanical pressure (see Rajagopal [27] for a discussion of the notion of pressure):

$$p=-\frac{\mathrm{tr}\mathbf{T}}{3}, \tag{3}$$

and hence, the terms in which the lambdas appear are pressure dependent. We also note that the term multiplying the identity tensor on the right-hand side of (2) has terms involving the trace of the linearized strain, which in virtue of the balance of mass implies dependence on the density. Thus, the constitutive relation (2) can be viewed as describing a body that has material moduli depending on both pressure and density. Such constitutive relations are well suited to describe porous bodies.

To derive from (2) a particular model more amenable to mathematical analysis, we make the assumptions below. Such assumptions allow us to gainfully exploit properties of ellipticity and boundedness, and hence, we obtain restrictions on the coefficients. Decomposing tensors into the deviatoric and spherical parts:

$$\mathbf{T}=\mathbf{T}^{*}+\frac{1}{3}(\mathrm{tr}\mathbf{T})\mathbf{I},\ \boldsymbol{\varepsilon}=\boldsymbol{\varepsilon}^{*}+\frac{1}{3}(\mathrm{tr}\boldsymbol{\varepsilon})\mathbf{I},\ \dot{\boldsymbol{\varepsilon}}=\dot{\boldsymbol{\varepsilon}}^{*}+\frac{1}{3}(\mathrm{tr}\dot{\boldsymbol{\varepsilon}})\mathbf{I}, \tag{4}$$

we assume that the nonlinearity in the deviatoric part of (2) is negligible, for example, under isotropic extension or compression studied in Section 4, such that

$$\alpha_1\boldsymbol{\varepsilon}^{*}+\alpha_2\dot{\boldsymbol{\varepsilon}}^{*}=\mathbf{T}^{*},\ \alpha_1(1+\lambda_1\mathrm{tr}\mathbf{T})\mathrm{tr}\boldsymbol{\varepsilon}+\alpha_2(1+\lambda_2\mathrm{tr}\mathbf{T})\mathrm{tr}\dot{\boldsymbol{\varepsilon}}=\mathrm{tr}\mathbf{T}+3(\alpha_3\mathrm{tr}\boldsymbol{\varepsilon}+\alpha_4\mathrm{tr}\dot{\boldsymbol{\varepsilon}}). \tag{5}$$

Furthermore, we assume that $\alpha_1\neq 0$, $\alpha_2\neq 0$, $\alpha_1-3\alpha_3\neq 0$, $\alpha_2-3\alpha_4\neq 0$, and the following two relations hold between the moduli:

$$\frac{\alpha_1}{\alpha_1-3\alpha_3}=\frac{\alpha_2}{\alpha_2-3\alpha_4}=:a,\ \frac{\alpha_1\lambda_1}{\alpha_1-3\alpha_3}=\frac{\alpha_2\lambda_2}{\alpha_2-3\alpha_4}=:b, \tag{6}$$

which reduces (5) to

$$\alpha_1\boldsymbol{\varepsilon}^{*}+\alpha_2\dot{\boldsymbol{\varepsilon}}^{*}=\mathbf{T}^{*},\ \frac{1}{a}(1+b\mathrm{tr}\mathbf{T})(\alpha_1\mathrm{tr}\boldsymbol{\varepsilon}+\alpha_2\mathrm{tr}\dot{\boldsymbol{\varepsilon}})=\mathrm{tr}\mathbf{T}. \tag{7}$$

Hereafter, we consider the model (7) and assume that parameters α_1, α_2, a, b satisfying $a\neq 0$ are independent. Now, the second equation in (7) is invertible and can be divided by $1+b\mathrm{tr}\mathbf{T}\neq 0$, because both $1+b\mathrm{tr}\mathbf{T}=0$ and $\mathrm{tr}\mathbf{T}=0$ in (7) lead to a contradiction.

However, it can be observed in (7) that small $1+b\mathrm{tr}\mathbf{T}$ implies $\alpha_1\mathrm{tr}\boldsymbol{\varepsilon}+\alpha_2\mathrm{tr}\dot{\boldsymbol{\varepsilon}}$ becoming unlimited. To be consistent with the assumption of small displacement gradient and its time derivative to be bounded, we apply a thresholding approach used by Itou et al. [5, 6]. For prescribed thresholds,

$$0<\underline{M}\le 1\le\overline{M}, \tag{8}$$

where $\underline{M}$ may be small, and the corresponding cut-off function

$$\overline{\underline{M}}[1+b\mathrm{tr}\mathbf{T}]:=\begin{cases}\underline{M}, & \text{if } 1+b\mathrm{tr}\mathbf{T}<\underline{M}\\ 1+b\mathrm{tr}\mathbf{T}, & \text{if } \underline{M}\le 1+b\mathrm{tr}\mathbf{T}\le\overline{M}\\ \overline{M}, & \text{if } 1+b\mathrm{tr}\mathbf{T}>\overline{M}\end{cases}, \tag{9}$$

we suggest the following threshold for equation (7):

$$\alpha_1\boldsymbol{\varepsilon}^*+\alpha_2\dot{\boldsymbol{\varepsilon}}^*=\mathbf{T}^*,\ \frac{1}{a}\overline{\underline{M}}[1+b\mathrm{tr}\mathbf{T}]\,(\alpha_1\mathrm{tr}\boldsymbol{\varepsilon}+\alpha_2\mathrm{tr}\dot{\boldsymbol{\varepsilon}})=\mathrm{tr}\mathbf{T}. \tag{10}$$

This implies that the nonlinear equation (7) holds if $\underline{M}\le 1+b\mathrm{tr}\mathbf{T}\le\overline{M}$ in (9). Otherwise, the linearized viscoelastic relations hold if either $1+b\mathrm{tr}\mathbf{T}<\underline{M}$, then

$$\alpha_1\boldsymbol{\varepsilon}^*+\alpha_2\dot{\boldsymbol{\varepsilon}}^*=\mathbf{T}^*,\ \frac{M}{a}\,(\alpha_1\mathrm{tr}\boldsymbol{\varepsilon}+\alpha_2\mathrm{tr}\dot{\boldsymbol{\varepsilon}})=\mathrm{tr}\mathbf{T}, \tag{11}$$

or $1+b\mathrm{tr}\mathbf{T}>\overline{M}$, then

$$\alpha_1\boldsymbol{\varepsilon}^*+\alpha_2\dot{\boldsymbol{\varepsilon}}^*=\mathbf{T}^*,\ \frac{\overline{M}}{a}\,(\alpha_1\mathrm{tr}\boldsymbol{\varepsilon}+\alpha_2\mathrm{tr}\dot{\boldsymbol{\varepsilon}})=\mathrm{tr}\mathbf{T}. \tag{12}$$

In our further considerations, we rely on the approximation (10).

Equation (10) includes the standard models such as the linearized constitutive relation. If $b=0$, then $\overline{\underline{M}}\equiv 1$ in (9) in virtue of (8), and from (10) and (4), we obtain the linear equation

$$\alpha_1\boldsymbol{\varepsilon}+\alpha_2\dot{\boldsymbol{\varepsilon}}=\mathbf{T}^*+\frac{1}{3}a\mathrm{tr}\mathbf{T}. \tag{13}$$

In particular, when $a=1$, relation (13) implies the linearized compressible Kelvin–Voigt model

$$\alpha_1\boldsymbol{\varepsilon}+\alpha_2\dot{\boldsymbol{\varepsilon}}=\mathbf{T}, \tag{14}$$

with the shear modulus α_1 and the viscosity α_2. If $b=0$ and $\alpha_2=0$ in (10), then we recover the constitutive equation for isotropic elasticity

$$\alpha_1\boldsymbol{\varepsilon}=\mathbf{T}+\alpha_1\left(\frac{1}{3}-\frac{1}{3a}\right)\mathrm{tr}\boldsymbol{\varepsilon}\mathbf{I}, \tag{15}$$

such that the moduli are determined using the Lamé parameters λ and μ as

$$\alpha_1=2\mu=\frac{E}{1+\nu},\ \alpha_1\frac{a-1}{3a}=-\lambda=-\frac{2\mu\nu}{1-2\nu},\ a=\frac{1-2\nu}{1+\nu}, \tag{16}$$

where the Young's modulus $E>0$ and Poisson's ratio $\nu\in(0,0.5)$. Thus, the parameters $\alpha_1>0$ and $a>0$ in (10) are given by (16), $\alpha_2>0$ is the viscosity, and b together with thresholds $\underline{M},\overline{M}$ satisfying (8) are free model parameters.

From the mathematical point of view, relations (10) define a time-dependent graph $\mathfrak{G}$ between $\mathbf{T}$ and $\alpha_1\boldsymbol{\varepsilon}+\alpha_2\dot{\boldsymbol{\varepsilon}}$. The theory of graphs is well suited to study implicit and multi-valued functions. Following the arguments by Bulíček et al. [28, 29], we will prove that $\mathfrak{G}$ is maximal monotone and coercive, thus providing existence of a solution for the proposed mixed variational problem. The concept of maximal monotony for nonlinear operators is exploited by Browder [30] and Minty

[31]. We cite the relevant results using pseudo-monotone operators in Itou et al. [32] and hemi-variational inequalities in Kovtunenko [33] and Sofonea and Migórski [34].

The structure of the paper is the following. In Section 2, we propose a parabolic mixed variational problem with respect to unknown $(\mathbf{T}, \boldsymbol{\varepsilon}, \dot{\boldsymbol{\varepsilon}})$ describing a nonlinear Kelvin–Voigt model by the thresholded equation (10). We prove its well-posedness in Section 3 based on the use maximal monotone graphs $\mathfrak{G}$. Finally, in Section 4, we present the example of isotropic extension or compression. In this example, an analytic solution for the Kelvin–Voigt problem is given when controlled by the pressure. The numerical simulation presented under cyclic pressure loading–unloading demonstrates the creep that such bodies exhibit. The solution for the thresholded model (10), unlike the prototype viscoelastic model (2), does not blow up under finite pressure when the loading is monotone. Moreover, the thresholded model also allows for the material moduli to be pressure dependent, which is not a possibility in the case of a simple material (see Noll [35]) of which the Kelvin–Voigt constitutive relation is a sub-class.

2 | A GENERALIZED KELVIN–VOIGT PROBLEM

Let Ω be a bounded domain in an Euclidean space $\mathbb{R}^3$ with Lipschitz continuous boundary $\partial\Omega$ and the unit normal vector $\mathbf{n} = (n_1, n_2, n_3)$ which is directed outward. Let the boundary be comprised of two disjoint sets $\partial\Omega = \overline{\Gamma_{\rm N}} \cup \overline{\Gamma_{\rm D}}$ corresponding to the Neumann $\Gamma_{\rm N}$ and nonempty Dirichlet $\Gamma_{\rm D}$ parts. For spatial points $\mathbf{x} = (x_1, x_2, x_3)$ in the closure $\overline{\Omega} = \Omega \cup \partial\Omega$ and times $t \in [0, T)$ with some final time $T > 0$ fixed, the right time-space cylinder will be denoted by $\Omega^T = (0, T) \times \Omega$ with the side consisting of two parts $\Gamma_{\rm N}^T = (0, T) \times \Gamma_{\rm N}$ and $\Gamma_{\rm D}^T = (0, T) \times \Gamma_{\rm D}$.

We look for the displacement vector $\mathbf{u} = (u_1, u_2, u_3)(t, \mathbf{x})$ in $[0, T) \times \overline{\Omega}$. In the space $\mathbb{R}^{3\times3}_{\rm sym}$ of second order symmetric 3-by-3 tensors, the displacement determines the linearized strain $\boldsymbol{\varepsilon} = \{\varepsilon_{ij}\}_{i,j=1}^3(t, \mathbf{x})$ through

$$\varepsilon_{ij}(\mathbf{u}) = \frac{1}{2}\left(\frac{\partial u_i}{\partial x_j} + \frac{\partial u_j}{\partial x_i}\right), \ i, j = 1, 2, 3, \tag{17}$$

and its time rate $\dot{\boldsymbol{\varepsilon}} = \{\dot{\varepsilon}_{ij}\}_{i,j=1}^3(t, \mathbf{x})$ through

$$\dot{\varepsilon}_{ij}(\mathbf{u}) = \frac{1}{2}\left(\frac{\partial \dot{u}_i}{\partial x_j} + \frac{\partial \dot{u}_j}{\partial x_i}\right), \ i, j = 1, 2, 3. \tag{18}$$

Let the body force $\mathbf{f} = (f_1, f_2, f_3)(t, \mathbf{x}) \in L^2(\Omega^T; \mathbb{R}^3)$ and the boundary traction $\mathbf{g} = (g_1, g_2, g_3)(t, \mathbf{x}) \in L^2(\Gamma_{\rm N}^T; \mathbb{R}^3)$ be given. On neglecting inertia, the Cauchy stress tensor $\mathbf{T} = \{T_{ij}\}_{i,j=1}^3(t, \mathbf{x}) \in \mathbb{R}^{3\times3}_{\rm sym}$ satisfies the quasi-static equilibrium equation

$$-\sum_{j=1}^{3} \frac{\partial T_{ij}}{\partial x_j} = f_i, \ i = 1, 2, 3, \ \text{in } \Omega^T. \tag{19}$$

We consider (19) with the standard, mixed Dirichlet–Neumann boundary conditions

$$\mathbf{u} = \mathbf{0} \text{ on } \Gamma_{\rm D}^T, \tag{20}$$

$$\mathbf{Tn} = \mathbf{g} \text{ on } \Gamma_{\rm N}^T, \tag{21}$$

where the traction at the boundary is given by $\mathbf{Tn} = \left\{\sum_{j=1}^3 T_{ij} n_j\right\}_{i=1}^3$. For the strain rate in (18), we should impose the initial condition at $t = 0$:

$$\mathbf{u}(0) = \mathbf{u}^0 \text{ in } \Omega, \tag{22}$$

given $\mathbf{u}^0 \in H^1(\Omega; \mathbb{R}^3)$ and $\mathbf{u}^0 = \mathbf{0}$ on $\Gamma_{\rm D}$. The evolutionary equilibrium problem (17)–(22) is completed with a constitutive relation between the strain, its rate, and stress which can be expressed in the implicit way of the inclusion relation on a graph in $(\mathbb{R}^{3\times3}_{\rm sym})^3$:

$$(\mathbf{T}, \boldsymbol{\varepsilon}, \dot{\boldsymbol{\varepsilon}}) \in \mathfrak{G}(0, T), \tag{23}$$

in which $\mathfrak{G}$ is the specified constitutive relation.

Based on the response approximation (10), deviatoric–spherical decomposition of tensors (4), and cut-off function $\overline{M}$ in (9), we introduce the time-dependent graph $\mathfrak{G} : (0,T) \mapsto (\mathbb{R}^{3\times3}_{\rm sym})^3$ in (23) as follows:

$$(\mathbf{T},\boldsymbol{\varepsilon},\dot{\boldsymbol{\varepsilon}}) \in \mathfrak{G}(0,T) \Longleftrightarrow \text{for all } t \in (0,T)\ \alpha_1\boldsymbol{\varepsilon}^* + \alpha_2\dot{\boldsymbol{\varepsilon}}^* = \mathbf{T}^*,\ \frac{1}{a}\underline{M}[1+b\mathrm{tr}\mathbf{T}]\,(\alpha_1\mathrm{tr}\boldsymbol{\varepsilon} + \alpha_2\mathrm{tr}\dot{\boldsymbol{\varepsilon}}) = \mathrm{tr}\mathbf{T}. \tag{24}$$

Here and hereafter, we assume $a>0$, $\alpha_1>0$, $\alpha_2>0$, free parameters $b\in\mathbb{R}$, $\underline{M}$ and $\overline{M}$ satisfying (8).

Lemma 1 (Properties of $\mathfrak{G}(0,T)$)**.** *The time-dependent graph in (24)*

$$\textit{includes the origin: } (\mathbf{0},\mathbf{0},\mathbf{0}) \in \mathfrak{G}(0,T). \tag{25}$$

For all tensors $(\mathbf{T},\boldsymbol{\varepsilon},\dot{\boldsymbol{\varepsilon}}) \in \mathfrak{G}(0,T)$, the graph is coercive with the uniform estimate:

$$\int_0^\tau (\alpha_1\boldsymbol{\varepsilon} + \alpha_2\dot{\boldsymbol{\varepsilon}})\cdot\mathbf{T}\,dt \geq C(a)\int_0^\tau \|\mathbf{T}\|^2\,dt + C\left(\underline{M}\right)\left(\int_0^\tau \left(\alpha_1^2\|\boldsymbol{\varepsilon}\|^2 + \alpha_2^2\|\dot{\boldsymbol{\varepsilon}}\|^2\right)\,dt + \alpha_1\alpha_2\left(\|\boldsymbol{\varepsilon}(\tau)\|^2 - \|\boldsymbol{\varepsilon}(0)\|^2\right)\right), \tag{26}$$

for all times $\tau\in(0,T)$, where the constant $C(a)$ and $C\left(\underline{M}\right)$ are defined by

$$C(\xi) := \frac{1}{2}\min\left(1, \frac{\xi^2}{a\overline{M}}\right) \textit{ for } \xi\in\mathbb{R}, \tag{27}$$

and using the Frobenius norm $\|\mathbf{T}\| = \sqrt{\mathbf{T}\cdot\mathbf{T}}$, where the dot implies the scalar product of tensors, for example, $\boldsymbol{\varepsilon}\cdot\mathbf{T} = \sum_{i,j=1}^3 \varepsilon_{ij}T_{ij}$. The graph is monotone:

$$\left[\alpha_1(\boldsymbol{\varepsilon}^1-\boldsymbol{\varepsilon}^2) + \alpha_2(\dot{\boldsymbol{\varepsilon}}^1-\dot{\boldsymbol{\varepsilon}}^2)\right]\cdot(\mathbf{T}^1-\mathbf{T}^2) \geq 0 \tag{28}$$

holds for all pairs $(\mathbf{T}^1,\boldsymbol{\varepsilon}^1,\dot{\boldsymbol{\varepsilon}}^1), (\mathbf{T}^2,\boldsymbol{\varepsilon}^2,\dot{\boldsymbol{\varepsilon}}^2) \in \mathfrak{G}(0,T)$, moreover, maximal monotone: for some $(\mathbf{T}^1,\boldsymbol{\varepsilon}^1,\dot{\boldsymbol{\varepsilon}}^1) \in (\mathbb{R}^{3\times3}_{sym})^3$,

$$\textit{if } \left[\alpha_1(\boldsymbol{\varepsilon}^1-\boldsymbol{\varepsilon}^2) + \alpha_2(\dot{\boldsymbol{\varepsilon}}^1-\dot{\boldsymbol{\varepsilon}}^2)\right]\cdot(\mathbf{T}^1-\mathbf{T}^2) \geq 0 \textit{ for all } (\mathbf{T}^2,\boldsymbol{\varepsilon}^2,\dot{\boldsymbol{\varepsilon}}^2) \in \mathfrak{G}(0,T), \textit{ then } (\mathbf{T}^1,\boldsymbol{\varepsilon}^1,\dot{\boldsymbol{\varepsilon}}^1) \in \mathfrak{G}(0,T). \tag{29}$$

Proof. Since the cut-off function $\overline{M} > 0$ according to (8) and (9), we can divide by $\underline{M}[1+b\mathrm{tr}\mathbf{T}]$ the last equation in (24). In this way, using the deviatoric–spherical decomposition of tensors (4), from (24), we derive the explicit relation

$$\alpha_1\boldsymbol{\varepsilon} + \alpha_2\dot{\boldsymbol{\varepsilon}} = \mathbf{T}^* + \frac{1}{3}\mathcal{F}[\mathrm{tr}\mathbf{T}]\mathbf{I}, \tag{30}$$

with the thresholding function

$$\mathcal{F}[\mathrm{tr}\mathbf{T}] := \frac{a\mathrm{tr}\mathbf{T}}{\underline{M}[1+b\mathrm{tr}\mathbf{T}]} = \begin{cases} \frac{a}{\underline{M}}\mathrm{tr}\mathbf{T}, & \text{if } 1+b\mathrm{tr}\mathbf{T} < \underline{M} \\ \frac{a\mathrm{tr}\mathbf{T}}{1+b\mathrm{tr}\mathbf{T}}, & \text{if } \underline{M} \leq 1+b\mathrm{tr}\mathbf{T} \leq \overline{M} \\ \frac{a}{\overline{M}}\mathrm{tr}\mathbf{T}, & \text{if } 1+b\mathrm{tr}\mathbf{T} > \overline{M} \end{cases}. \tag{31}$$

Using differentiation, the function $\mathcal{F} : \mathbb{R}\mapsto\mathbb{R}$ in (31) is Lipschitz continuous:

$$\left|\mathcal{F}[\mathrm{tr}\mathbf{T}^1] - \mathcal{F}[\mathrm{tr}\mathbf{T}^2]\right| \leq \frac{a}{\underline{M}^2}\left|\mathrm{tr}(\mathbf{T}^1-\mathbf{T}^2)\right|, \tag{32}$$

for all $\mathbf{T}^1,\mathbf{T}^2\in\mathbb{R}^{3\times3}_{\rm sym}$, and strongly monotone:

$$\left(\mathcal{F}[\mathrm{tr}\mathbf{T}^1] - \mathcal{F}[\mathrm{tr}\mathbf{T}^2]\right)\mathrm{tr}(\mathbf{T}^1-\mathbf{T}^2) \geq \frac{a}{\overline{M}^2}\mathrm{tr}^2(\mathbf{T}^1-\mathbf{T}^2). \tag{33}$$

Directly from (31) boundedness follows:

$$|\mathcal{F}[\mathrm{tr}\mathbf{T}]| \le \frac{a}{\underline{M}}|\mathrm{tr}\mathbf{T}|$$

and coercivity:

$$\mathcal{F}[\mathrm{tr}\mathbf{T}]\mathrm{tr}\mathbf{T} \ge \frac{a}{\overline{M}}\mathrm{tr}^2\mathbf{T}.$$

Forming the scalar product of (30) with the stress $\mathbf{T}$, using the upper and lower bounds, then expressing $\mathbf{T}$ from (30), we obtain

$$\begin{aligned}(\alpha_1\boldsymbol{\varepsilon}+\alpha_2\dot{\boldsymbol{\varepsilon}})\cdot\mathbf{T} &= \|\mathbf{T}^*\|^2+\frac{1}{3}\mathcal{F}[\mathrm{tr}\mathbf{T}]\mathrm{tr}\mathbf{T} \ge \|\mathbf{T}^*\|^2+\frac{a}{3\overline{M}}\mathrm{tr}^2\mathbf{T}\\ &\ge \frac{1}{2}\left(\|\mathbf{T}^*\|^2+\|\alpha_1\boldsymbol{\varepsilon}^*+\alpha_2\dot{\boldsymbol{\varepsilon}}^*\|^2\right)+\frac{a}{6\overline{M}}\left(\mathrm{tr}^2\mathbf{T}+\left(\frac{\overline{M}}{a}\mathcal{F}[\mathrm{tr}\mathbf{T}]\right)^2\right)\\ &\ge \frac{1}{2}\min\left(1,\frac{a}{\overline{M}}\right)\left(\|\mathbf{T}^*\|^2+\frac{1}{3}\mathrm{tr}^2\mathbf{T}\right)+\frac{1}{2}\min\left(1,\frac{\overline{M}^2}{a\overline{M}}\right)\left(\|\alpha_1\boldsymbol{\varepsilon}^*+\alpha_2\dot{\boldsymbol{\varepsilon}}^*\|^2+\frac{1}{3}\mathrm{tr}^2(\alpha_1\boldsymbol{\varepsilon}+\alpha_2\dot{\boldsymbol{\varepsilon}})\right).\end{aligned}$$

After rearranging the terms, using the norm identity $\|\mathbf{T}\|^2=\|\mathbf{T}^*\|^2+\mathrm{tr}^2\mathbf{T}/3$ for the decomposition (4) and using the notation (27), the following inequality holds:

$$(\alpha_1\boldsymbol{\varepsilon}+\alpha_2\dot{\boldsymbol{\varepsilon}})\cdot\mathbf{T} \ge C(a)\|\mathbf{T}\|^2+C\left(\underline{M}\right)\left(\alpha_1^2\|\boldsymbol{\varepsilon}\|^2+\alpha_2^2\|\dot{\boldsymbol{\varepsilon}}\|^2+2\alpha_1\alpha_2(\boldsymbol{\varepsilon}\cdot\dot{\boldsymbol{\varepsilon}})\right). \tag{34}$$

The integration of (34) over $t\in(0,\tau)$ for arbitrarily fixed time $\tau\in(0,T)$ with the help of the chain rule $d(\|\boldsymbol{\varepsilon}\|^2)/dt=2\boldsymbol{\varepsilon}\cdot\dot{\boldsymbol{\varepsilon}}$ results in the lower estimate (26).

For two points on the graph $(\mathbf{T}^1,\boldsymbol{\varepsilon}^1,\dot{\boldsymbol{\varepsilon}}^1),(\mathbf{T}^2,\boldsymbol{\varepsilon}^2,\dot{\boldsymbol{\varepsilon}}^2)\in\mathfrak{G}(0,T)$, this implies that relation (30) holds between their coordinates:

$$\alpha_1\boldsymbol{\varepsilon}^n+\alpha_2\dot{\boldsymbol{\varepsilon}}^n=(\mathbf{T}^n)^*+\frac{1}{3}\mathcal{F}[\mathrm{tr}\mathbf{T}^n]\mathbf{I},\ \ n=1,2. \tag{35}$$

Subtracting (35) for $n=1$ and $n=2$, we form the corresponding scalar product

$$\left[\alpha_1(\boldsymbol{\varepsilon}^1-\boldsymbol{\varepsilon}^2)+\alpha_2(\dot{\boldsymbol{\varepsilon}}^1-\dot{\boldsymbol{\varepsilon}}^2)\right]\cdot(\mathbf{T}^1-\mathbf{T}^2)=\|(\mathbf{T}^1-\mathbf{T}^2)^*\|^2+\frac{1}{3}\left(\mathcal{F}[\mathrm{tr}\mathbf{T}^1]-\mathcal{F}[\mathrm{tr}\mathbf{T}^2]\right)\mathrm{tr}(\mathbf{T}^1-\mathbf{T}^2)\ge\min\left(1,\frac{a}{\overline{M}^2}\right)\|\mathbf{T}^1-\mathbf{T}^2\|^2,$$

which is estimated as a consequence of the strong monotony of $\mathcal{F}$ in (33). Thus, the monotone property (28) is justified for $\mathfrak{G}(0,T)$.

Now, for some $(\mathbf{T}^1,\boldsymbol{\varepsilon}^1,\dot{\boldsymbol{\varepsilon}}^1)\in(\mathbb{R}^{3\times3}_{\mathrm{sym}})^3$, let the inequality in (29) hold for all $(\mathbf{T}^2,\boldsymbol{\varepsilon}^2,\dot{\boldsymbol{\varepsilon}}^2)\in\mathfrak{G}(0,T)$, that satisfies (35). For arbitrary $\mathbf{T}\in\mathbb{R}^{3\times3}_{\mathrm{sym}}$ and small $\delta>0$, we set $\mathbf{T}^\delta=\mathbf{T}^1\pm\delta\mathbf{T}\in\mathbb{R}^{3\times3}_{\mathrm{sym}}$ and solve the first-order linear inhomogeneous ODE system with respect to $\boldsymbol{\varepsilon}^\delta\in\mathbb{R}^{3\times3}_{\mathrm{sym}}$:

$$\alpha_1\boldsymbol{\varepsilon}^\delta+\alpha_2\dot{\boldsymbol{\varepsilon}}^\delta=(\mathbf{T}^\delta)^*+\frac{1}{3}\mathcal{F}[\mathrm{tr}\mathbf{T}^\delta]\mathbf{I}, \tag{36}$$

which is called a selection with respect to the graph because $(\mathbf{T}^\delta,\boldsymbol{\varepsilon}^\delta,\dot{\boldsymbol{\varepsilon}}^\delta)\in\mathfrak{G}(0,T)$. Then, testing (29) with $(\mathbf{T}^2,\boldsymbol{\varepsilon}^2,\dot{\boldsymbol{\varepsilon}}^2)=(\mathbf{T}^\delta,\boldsymbol{\varepsilon}^\delta,\dot{\boldsymbol{\varepsilon}}^\delta)$ and inserting (36), we derive

$$0\le\left[\alpha_1(\boldsymbol{\varepsilon}^1-\boldsymbol{\varepsilon}^\delta)+\alpha_2(\dot{\boldsymbol{\varepsilon}}^1-\dot{\boldsymbol{\varepsilon}}^\delta)\right]\cdot(\mathbf{T}^1-\mathbf{T}^\delta)=\mp\delta\left(\alpha_1\boldsymbol{\varepsilon}^1+\alpha_2\dot{\boldsymbol{\varepsilon}}^1-(\mathbf{T}^1\pm\delta\mathbf{T})^*-\frac{1}{3}\mathcal{F}[\mathrm{tr}(\mathbf{T}^1\pm\delta\mathbf{T})]\mathbf{I}\right)\cdot\mathbf{T},$$

which after division by δ yields

$$\mp\left(\alpha_1\boldsymbol{\varepsilon}^1+\alpha_2\dot{\boldsymbol{\varepsilon}}^1-(\mathbf{T}^1)^*\mp\delta\mathbf{T}^*-\frac{1}{3}\mathcal{F}[\mathrm{tr}(\mathbf{T}^1\pm\delta\mathbf{T})]\mathbf{I}\right)\cdot\mathbf{T}\ge0.$$

On taking the limit as $\delta \to 0$, due to the continuity of $\mathcal{F}$ in (32) leads to the two opposite inequalities with the plus and minus signs providing the equality

$$\left(\alpha_1\boldsymbol{\varepsilon}^1 + \alpha_2\dot{\boldsymbol{\varepsilon}}^1 - (\mathbf{T}^1)^* - \frac{1}{3}\mathcal{F}[\mathrm{tr}\mathbf{T}^1]\mathbf{I}\right)\cdot\mathbf{T} = 0, \tag{37}$$

for all $\mathbf{T} \in \mathbb{R}^{3\times3}_{\mathrm{sym}}$. The variational equation (37) implies that (35) holds for $(\mathbf{T}^1, \boldsymbol{\varepsilon}^1, \dot{\boldsymbol{\varepsilon}}^1)$. Hence, $(\mathbf{T}^1, \boldsymbol{\varepsilon}^1, \dot{\boldsymbol{\varepsilon}}^1) \in \mathfrak{G}(0, T)$ according to the definition of the graph (24), thus fulfilling the maximal monotone property (29).

The assertion (25) is evident. The proof is completed. □

Next, we state a variational formulation for the parabolic–elliptic problem (17)–(22) and (24). After forming the scalar product of the equilibrium equation (19) with $\mathbf{v} = (v_1, v_2, v_3)(x)$ and integration by parts over the time-space cylinder Ω^T with the help of the well-known Green's formula, we obtain

$$-\int_\Omega \sum_{i,j=1}^{3} \frac{\partial T_{ij}}{\partial x_j} v_i \, d\mathbf{x} = \int_\Omega \mathbf{T}\cdot\boldsymbol{\varepsilon}(\mathbf{v})\, d\mathbf{x} - \int_{\partial\Omega} \mathbf{T}\mathbf{n}\cdot\mathbf{v}\, dS_{\mathbf{x}},$$

where $\boldsymbol{\varepsilon}(\mathbf{v})$ is defined according to (17), and using the Neumann boundary condition (21), we arrive at

$$\int_{\Omega^T} \mathbf{T}\cdot\boldsymbol{\varepsilon}(\mathbf{v})\, d\mathbf{x}dt = \int_{\Omega^T} \mathbf{f}\cdot\mathbf{v}\, d\mathbf{x}dt + \int_{\Gamma_{\mathrm{N}}^T} \mathbf{g}\cdot\mathbf{v}\, dS_{\mathbf{x}}dt, \tag{38}$$

for all test functions $\mathbf{v} \in H^1(\Omega;\mathbb{R}^3)$ such that $\mathbf{v} = \mathbf{0}$ on Γ_{D}. Conversely, if $\mathbf{x} \mapsto \mathbf{T}$ is H^1-smooth, then pointwise relations (19) and (21) follow from (38).

We make a selection on the graph $\mathfrak{G}(0, T)$ for the stress $\mathbf{T} \in L^2(\Omega^T;\mathbb{R}^{3\times3}_{\mathrm{sym}})$, linearized strain (17) and its rate (18) determined by the displacement $\mathbf{u} \in H^1(0, T; H^1(\Omega;\mathbb{R}^3))$ such that $\mathbf{u} = \mathbf{0}$ on Γ_{D}^T, which fulfill the inclusion in (24) in the weak form:

$$\begin{aligned}(\mathbf{T}, \boldsymbol{\varepsilon}(\mathbf{u}), \dot{\boldsymbol{\varepsilon}}(\mathbf{u})) \in \mathfrak{G}(0, T) \Longleftrightarrow \int_{\Omega^T} (\boldsymbol{\varepsilon}(\alpha_1\mathbf{u} + \alpha_2\dot{\mathbf{u}}) - \mathbf{T})^* \cdot \boldsymbol{\eta}^* \, d\mathbf{x}dt = 0,\\ \int_{\Omega^T} \left(\frac{1}{a}\underline{M}[1 + b\mathrm{tr}\mathbf{T}]\mathrm{tr}\boldsymbol{\varepsilon}(\alpha_1\mathbf{u} + \alpha_2\dot{\mathbf{u}}) - \mathrm{tr}\mathbf{T}\right)\mathrm{tr}\boldsymbol{\eta}\, d\mathbf{x}dt = 0\end{aligned} \tag{39}$$

for all test functions $\boldsymbol{\eta} \in L^2(\Omega;\mathbb{R}^{3\times3}_{\mathrm{sym}})$.

A weak solution satisfying the variational relations (38) and (39) will be provided in the next section.

3 | WELL-POSEDNESS ANALYSIS BASED ON MAXIMAL MONOTONE GRAPHS

We begin with preliminaries: the well-known Korn–Poincaré inequality

$$\|\boldsymbol{\varepsilon}(\mathbf{u})\|_{L^2(\Omega)} \le \|\mathbf{u}\|_{H^1(\Omega)} \le C_{\mathrm{KP}}\|\boldsymbol{\varepsilon}(\mathbf{u})\|_{L^2(\Omega)} \text{ if } \mathbf{u} = \mathbf{0} \text{ on } \Gamma_{\mathrm{D}}, \tag{40}$$

and the theorem on boundary trace

$$\|\mathbf{u}\|_{L^2(\partial\Omega)} \le C_{\mathrm{tr}}\|\mathbf{u}\|_{H^1(\Omega)}. \tag{41}$$

Theorem 1 (Existence of solution)**.** *The weak solution* $\mathbf{T} \in L^2(\Omega^T;\mathbb{R}^{3\times3}_{sym})$ *and* $\mathbf{u} \in H^1(0, T; H^1(\Omega;\mathbb{R}^3))$ *satisfying the Dirichlet boundary condition (20), initial condition (22), and variational relations (38) and (39) exists, it is unique and fulfills the following a priori estimate:*

$$\begin{aligned}C(a)\|\mathbf{T}\|^2_{L^2(\Omega^T)} + \frac{C\left(\underline{M}\right)}{2C_{KP}^2}\Big(\alpha_1^2\|\mathbf{u}\|^2_{L^2(0,T;H^1(\Omega))} + \alpha_2^2\|\dot{\mathbf{u}}\|^2_{L^2(0,T;H^1(\Omega))}\\ + 2\alpha_1\alpha_2\|\mathbf{u}\|^2_{L^\infty(0,T;H^1(\Omega))}\Big) \le C\left(\underline{M}\right)\alpha_1\alpha_2\|\mathbf{u}^0\|^2_{H^1(\Omega)} + \frac{C_{KP}^2}{C\left(\underline{M}\right)}C^2(\mathbf{f}, \mathbf{g}),\end{aligned} \tag{42}$$

where $C(a)$ and $C\left(\underline{M}\right)$ are defined in (27), and the prescribed forces determine

$$C(\mathbf{f},\mathbf{g}) := \|\mathbf{f}\|_{L^2(\Omega^T)} + C_{tr}\|\mathbf{g}\|_{L^2(\Gamma_{\mathrm{N}}^T)}. \tag{43}$$

We remark that $\|\mathbf{u}\|_{L^\infty(0,T;H^1(\Omega))}$ can be skipped in the estimate (42) since it is bounded by the stronger norm $\|\mathbf{u}\|_{H^1(0,T;H^1(\Omega))}$ in virtue of the continuous embedding.

Proof. We prove the assertion in three subsequent steps: Galerkin approximation, uniform estimate, and passage to the limit.

Galerkin approximation

Let a sequence of subspaces $S^k = \mathrm{span}\{\boldsymbol{\eta}^m\}_{m=1}^k$ and $V^k = \mathrm{span}\{\mathbf{v}^m\}_{m=1}^k$ of finite dimensions $k \in \mathbb{N}$ build the conforming approximation of the admissible stress $\mathbf{T}$ and displacement $\mathbf{u}$ preserving $\mathbf{u} = \mathbf{0}$ on Γ_{D}. We assume that $\cup_{k=1}^\infty S^k$ is dense in $L^2(\Omega;\mathbb{R}^{3\times3}_{\mathrm{sym}})$, the union $\cup_{k=1}^\infty V^k$ is dense in $H^1(\Omega;\mathbb{R}^3)$, and $\mathbf{v}^m \in V^k$ implies $\boldsymbol{\varepsilon}(\mathbf{v}^m) \in S^k$.

We look for a weak solution $\mathbf{T}^k \in L^2(0,T;S^k)$ and $\mathbf{u}^k \in H^1(0,T;V^k)$ as

$$\mathbf{T}^k = \sum_{m=1}^k T_m^k(t)\boldsymbol{\eta}^m(\mathbf{x}),\ \mathbf{u}^k = \sum_{m=1}^k U_m^k(t)\mathbf{v}^m(\mathbf{x}), \tag{44}$$

satisfying the semi-discrete in space problem given in the variational form:

$$\int_{\Omega^T} \mathbf{T}^k \cdot \boldsymbol{\varepsilon}(\mathbf{v}^m)\,d\mathbf{x}dt = \int_{\Omega^T} \mathbf{f}\cdot\mathbf{v}^m\,d\mathbf{x}dt + \int_{\Gamma_{\mathrm{N}}^T} \mathbf{g}\cdot\mathbf{v}^m\,dS_{\mathbf{x}}dt, \tag{45}$$

which is endowed with the constitutive equation according to (30):

$$\int_{\Omega^T} \boldsymbol{\varepsilon}(\alpha_1\mathbf{u}^k + \alpha_2\dot{\mathbf{u}}^k)\cdot\boldsymbol{\eta}^m\,d\mathbf{x}dt = \int_{\Omega^T}\left((\mathbf{T}^k)^* + \frac{1}{3}\mathcal{F}[\mathrm{tr}\mathbf{T}^k]\mathbf{I}\right)\cdot\boldsymbol{\eta}^m\,d\mathbf{x}dt, \tag{46}$$

for all basis functions $\mathbf{v}^m \in V^k$ and $\boldsymbol{\eta}^m \in S^k$, under the initial condition

$$\mathbf{u}^k(0) = \sum_{m=1}^k U_m^k(0)\mathbf{v}^m,\ U_m^k(0) := \int_\Omega \mathbf{u}^0\cdot\mathbf{v}^m\,d\mathbf{x}. \tag{47}$$

Inserting the ansatz (44), the quasi-static system of Equations (45) and (46) can be solved with respect to the time-dependent coefficients T_m^k and $F_m^k := \alpha_1 U_m^k + \alpha_2\dot{U}_m^k$ by the Browder–Minty theorem, due to the Lipschitz continuity (32) and strong monotony (33) properties of the nonlinear function $\mathcal{F}$. Then, the coefficient $U_m^k \in H^1(0,T)$ solving the first-order ODE system $\alpha_1 U_m^k + \alpha_2\dot{U}_m^k = F_m^k$ can be written explicitly by the convolution Volterra integral:

$$U_m^k(t) = U_m^k(0)\exp\left(\frac{-\alpha_1 t}{\alpha_2}\right) + \frac{1}{\alpha_2}\int_0^t F_m^k(s)\exp\left(\frac{-\alpha_1(t-s)}{\alpha_2}\right)ds. \tag{48}$$

Uniform estimate

The stress $\mathbf{T} = \mathbf{T}^k$, strain $\boldsymbol{\varepsilon} = \boldsymbol{\varepsilon}(\mathbf{u}^k)$, and strain rate $\dot{\boldsymbol{\varepsilon}} = \boldsymbol{\varepsilon}(\dot{\mathbf{u}}^k)$ are connected by the constitutive equation (46), hence the selection $(\mathbf{T}^k, \boldsymbol{\varepsilon}(\mathbf{u}^k), \boldsymbol{\varepsilon}(\dot{\mathbf{u}}^k)) \in \mathfrak{G}(0,T)$. Therefore, we can apply the coercivity property (26) which holds on the graph. Integrating over domain Ω, taking the maximum over $\tau \in (0,T)$, and using the Korn–Poincaré inequality (40) yields the lower bound

$$\begin{aligned}\int_{\Omega^T} \boldsymbol{\varepsilon}(\alpha_1\mathbf{u}^k + \alpha_2\dot{\mathbf{u}}^k)\cdot\mathbf{T}^k\,d\mathbf{x}dt \geq C(a)\|\mathbf{T}^k\|^2_{L^2(\Omega^T)} - C\left(\underline{M}\right)\alpha_1\alpha_2\|\mathbf{u}^0\|^2_{H^1(\Omega)}\\ + \frac{C\left(\underline{M}\right)}{C_{\mathrm{KP}}^2}\left(\alpha_1^2\|\mathbf{u}^k\|^2_{L^2(0,T;H^1(\Omega))} + \alpha_2^2\|\dot{\mathbf{u}}^k\|^2_{L^2(0,T;H^1(\Omega))} + \alpha_1\alpha_2\|\mathbf{u}^k\|^2_{L^\infty(0,T;H^1(\Omega))}\right),\end{aligned} \tag{49}$$

with constant $C(a)$ and $C\left(\underline{M}\right)$ from (27). Here, the initial value $\mathbf{u}^k(0)$ was estimated by $\mathbf{u}^0$ in virtue of (47). On the other side, we test the variational equation (45) with $\mathbf{v}^m = \alpha_1\mathbf{u}^k + \alpha_2\dot{\mathbf{u}}^k$, apply the Cauchy–Schwarz, weighted Young, and trace (41) inequalities, which provide the upper bound with constant $C(\mathbf{f},\mathbf{g})$ from (43):

$$\begin{aligned}\int_{\Omega^T}\mathbf{T}^k\cdot\boldsymbol{\varepsilon}(\alpha_1\mathbf{u}^k+\alpha_2\dot{\mathbf{u}}^k)\,d\mathbf{x}dt &\le C(\mathbf{f},\mathbf{g})\|\alpha_1\mathbf{u}^k+\alpha_2\dot{\mathbf{u}}^k\|_{L^2(0,T;H^1(\Omega))}\\ \le \frac{C\left(\underline{M}\right)}{2C_{\mathrm{KP}}^2}\left(\alpha_1^2\|\mathbf{u}^k\|^2_{L^2(0,T;H^1(\Omega))}+\alpha_2^2\|\dot{\mathbf{u}}^k\|^2_{L^2(0,T;H^1(\Omega))}\right)&+\frac{C_{\mathrm{KP}}^2}{C\left(\underline{M}\right)}C^2(\mathbf{f},\mathbf{g}).\end{aligned}\tag{50}$$

Combining together (49) and (50) leads to the uniform estimate

$$\begin{aligned}C(a)\|\mathbf{T}^k\|^2_{L^2(\Omega^T)}+\frac{C\left(\underline{M}\right)}{2C_{\mathrm{KP}}^2}\Big(\alpha_1^2\|\mathbf{u}^k\|^2_{L^2(0,T;H^1(\Omega))}+\alpha_2^2\|\dot{\mathbf{u}}^k\|^2_{L^2(0,T;H^1(\Omega))}&\\ +2\alpha_1\alpha_2\|\mathbf{u}^k\|^2_{L^\infty(0,T;H^1(\Omega))}\Big)\le C\left(\underline{M}\right)\alpha_1\alpha_2\|\mathbf{u}^0\|^2_{H^1(\Omega)}+\frac{C_{\mathrm{KP}}^2}{C\left(\underline{M}\right)}C^2(\mathbf{f},\mathbf{g}).&\end{aligned}\tag{51}$$

Passage to the limit

On the basis of the boundedness (51), we conclude with a weakly convergent subsequence still denoted by k such that

$$\mathbf{T}^k\rightharpoonup\mathbf{T}\ \text{in}\ L^2(\Omega^T;\mathbb{R}^{3\times3}_{\mathrm{sym}}),\ \mathbf{u}^k\overset{\star}{\rightharpoonup}\mathbf{u}\ \text{in}\ L^\infty(0,T;H^1(\Omega;\mathbb{R}^3)),\ \dot{\mathbf{u}}^k\rightharpoonup\dot{\mathbf{u}}\ \text{in}\ L^2(0,T;H^1(\Omega;\mathbb{R}^3))\ \text{as}\ k\to\infty.\tag{52}$$

Taking the limit of the linear relations (45) and (47), we get the equilibrium equation (38) and initial condition (22) for $\mathbf{T}$ and $\mathbf{u}$ from (52). Next, we derive (39).

Testing the limit equation (38) with $\mathbf{v} = \alpha_1\mathbf{u} + \alpha_2\dot{\mathbf{u}}$, we find that

$$\int_{\Omega^T}\mathbf{T}\cdot\boldsymbol{\varepsilon}(\alpha_1\mathbf{u}+\alpha_2\dot{\mathbf{u}})\,d\mathbf{x}dt=\int_{\Omega^T}\mathbf{f}\cdot(\alpha_1\mathbf{u}+\alpha_2\dot{\mathbf{u}})\,d\mathbf{x}dt+\int_{\Gamma_{\mathrm{N}}^T}\mathbf{g}\cdot(\alpha_1\mathbf{u}+\alpha_2\dot{\mathbf{u}})\,dS_{\mathbf{x}}dt.\tag{53}$$

For finite k, using the ansatz (44) in (45) leads to

$$\int_{\Omega^T}\mathbf{T}^k\cdot\boldsymbol{\varepsilon}(\alpha_1\mathbf{u}^k+\alpha_2\dot{\mathbf{u}}^k)\,d\mathbf{x}dt=\int_{\Omega^T}\mathbf{f}\cdot(\alpha_1\mathbf{u}^k+\alpha_2\dot{\mathbf{u}}^k)\,d\mathbf{x}dt+\int_{\Gamma_{\mathrm{N}}^T}\mathbf{g}\cdot(\alpha_1\mathbf{u}^k+\alpha_2\dot{\mathbf{u}}^k)\,dS_{\mathbf{x}}dt.\tag{54}$$

By the virtue of weak convergences in (52), from (53) and (54), we conclude that

$$\lim_{k\to\infty}\int_{\Omega^T}\mathbf{T}^k\cdot\boldsymbol{\varepsilon}(\alpha_1\mathbf{u}^k+\alpha_2\dot{\mathbf{u}}^k)\,d\mathbf{x}dt=\int_{\Omega^T}\mathbf{T}\cdot\boldsymbol{\varepsilon}(\alpha_1\mathbf{u}+\alpha_2\dot{\mathbf{u}})\,d\mathbf{x}dt.\tag{55}$$

For arbitrary $(\mathbf{T}^2,\boldsymbol{\varepsilon}^2,\dot{\boldsymbol{\varepsilon}}^2)\in L^2(\Omega^T;\mathbb{R}^{3\times3}_{\mathrm{sym}})^3$ on the graph, using the monotony

$$\left[\boldsymbol{\varepsilon}(\alpha_1\mathbf{u}^k+\alpha_2\dot{\mathbf{u}}^k)-\alpha_1\boldsymbol{\varepsilon}^2-\alpha_2\dot{\boldsymbol{\varepsilon}}^2\right]\cdot(\mathbf{T}^k-\mathbf{T}^2)\ge0,$$

according to (28), we estimate from below the scalar product

$$\begin{aligned}&\int_{\Omega^T}\left[\boldsymbol{\varepsilon}(\alpha_1\mathbf{u}+\alpha_2\dot{\mathbf{u}})-\alpha_1\boldsymbol{\varepsilon}^2-\alpha_2\dot{\boldsymbol{\varepsilon}}^2\right]\cdot(\mathbf{T}-\mathbf{T}^2)\,d\mathbf{x}dt\\ &\ge\int_{\Omega^T}\left(\left[\boldsymbol{\varepsilon}(\alpha_1\mathbf{u}^k+\alpha_2\dot{\mathbf{u}}^k)-\alpha_1\boldsymbol{\varepsilon}^2-\alpha_2\dot{\boldsymbol{\varepsilon}}^2\right]\cdot(\mathbf{T}-\mathbf{T}^k)+\boldsymbol{\varepsilon}\left(\alpha_1\mathbf{u}+\alpha_2\dot{\mathbf{u}}-\alpha_1\mathbf{u}^k-\alpha_2\dot{\mathbf{u}}^k\right)\cdot(\mathbf{T}-\mathbf{T}^2)\right)d\mathbf{x}dt.\end{aligned}$$

The limit passage based on convergences in (52) and (55) leads to

$$\int_{\Omega^T}\left[\boldsymbol{\varepsilon}(\alpha_1\mathbf{u}+\alpha_2\dot{\mathbf{u}})-\alpha_1\boldsymbol{\varepsilon}^2-\alpha_2\dot{\boldsymbol{\varepsilon}}^2\right]\cdot(\mathbf{T}-\mathbf{T}^2)\,d\mathbf{x}dt\ge\limsup_{k\to\infty}\int_{\Omega^T}\boldsymbol{\varepsilon}(\alpha_1\mathbf{u}^k+\alpha_2\dot{\mathbf{u}}^k)\cdot(\mathbf{T}-\mathbf{T}^k)\,d\mathbf{x}dt=0.$$

Then, the maximal monotone property (29) of the graph guarantees that the limit functions from (52) fulfill $(\mathbf{T}, \boldsymbol{\varepsilon}(\mathbf{u}), \boldsymbol{\varepsilon}(\dot{\mathbf{u}})) \in \mathfrak{G}(0, T)$, hence (39) holds.

The uniqueness follows from the strong monotony of $\mathcal{F}$ in (33). This completes the proof. □

4 | SEMI-ANALYTICAL EXAMPLE OF ISOTROPIC, UNIFORM, EXTENSION, OR COMPRESSION

In this section, we simplify our consideration under the assumption of isotropic extension or compression when

$$\mathbf{T} = -p(t)\mathbf{I},\ \boldsymbol{\varepsilon} = \frac{1}{3}e(t)\mathbf{I},\ \dot{\boldsymbol{\varepsilon}} = \frac{1}{3}\dot{e}(t)\mathbf{I}. \tag{56}$$

Formula (56) implies that the deviatoric parts $\mathbf{T}^* = \boldsymbol{\varepsilon}^* = \dot{\boldsymbol{\varepsilon}}^* = \mathbf{0}$, and the unknown scalar functions are the pressure p (henceforth, by pressure, we refer to mechanical pressure) from (3) and the dilatation $e = \mathrm{tr}\boldsymbol{\varepsilon}$ according to the deviatoric–spherical decomposition (4). The sign $p < 0$ implies extension, and $p > 0$ compression. Since the stress, linearized strain, and rate of the linearized strain tensors are space independent by (56), the equilibrium equation (19) is satisfied identically with $\mathbf{f} \equiv \mathbf{0}$.

We will compare the underlying viscoelastic models introduced in Section 1. Under the assumption (56), the reference constitutive response (2) is equivalent to (7) given implicitly as

$$\frac{1}{a}(1 - 3bp)(\alpha_1 e + \alpha_2 \dot{e}) = -3p,$$

or after division by $1 - 3bp \neq 0$, explicitly with respect to e as

$$\alpha_1 e + \alpha_2 \dot{e} = \frac{-3ap}{1 - 3bp}. \tag{57}$$

The thresholding approximation (10) in its explicit form (30) using the thresholding function $\mathcal{F}$ from (31) reads

$$\alpha_1 e + \alpha_2 \dot{e} = \mathcal{F}[-3p] = \begin{cases} \frac{-3a}{\underline{M}}p, & \text{if } 1 - 3bp < \underline{M} \\ \frac{-3ap}{1-3bp}, & \text{if } \underline{M} \leq 1 - 3bp \leq \overline{M} \\ \frac{-3a}{\overline{M}}p, & \text{if } 1 - 3bp > \overline{M} \end{cases}. \tag{58}$$

For bounded $\underline{M} \leq 1 - 3bp \leq \overline{M}$, Equation (58) coincides with (57). In the case of interest, if $1 - 3bp < \underline{M}$, then (58) reduces to the linearized Kelvin–Voigt model

$$\alpha_1 e + \alpha_2 \dot{e} = \frac{-3a}{\underline{M}}p. \tag{59}$$

We study the stress-control case, namely, we look for the evolution of dilatation under time-dependent pressure. Let the pressure be prescribed by an affine function

$$p(t) = p_0 + g(t - t_0) \text{ for } t_0 \leq t \leq \tau, \tag{60}$$

with constant p_0 and g. Inserting (60) into (59), we form the right-hand side

$$F(t) = \frac{-3a}{\underline{M}}p(t) = F_0 + G_0(t - t_0),\ F_0 = \frac{-3a}{\underline{M}}p_0,\ G_0 = \frac{-3a}{\underline{M}}g, \tag{61}$$

and express a closed-form solution $e(t)$ to the linear first-order ODE (59) on the time interval $t \in [t_0, \tau]$ with the help of the convolution Volterra integral (48) as

$$\begin{aligned} e(t) &= e(t_0)\exp\left(\frac{-\alpha_1(t-t_0)}{\alpha_2}\right) + \frac{1}{\alpha_2}\int_{t_0}^{t} F(s)\exp\left(\frac{-\alpha_1(t-s)}{\alpha_2}\right) ds \\ &= \frac{1}{\alpha_1}\left[F_0 + G_0\left(t - t_0 - \frac{\alpha_2}{\alpha_1}\right) + \left(\alpha_1 e(t_0) - F_0 + G_0\frac{\alpha_2}{\alpha_1}\right)\exp\left(\frac{\alpha_1(t_0-t)}{\alpha_2}\right)\right]. \end{aligned} \tag{62}$$

For the nonlinear equation (57), we split $[t_0, \tau]$ by equidistant points $t_k = t_0 + k\delta t$ for $k = 0, 1, \dots, N$ into N intervals of the time step $\delta t = (\tau - t_0)/N$. The right-hand side $F(t) := -3ap(t)/(1 - 3bp(t))$ is approximated piecewise linearly by

$$F^N(t) = F_k + G_k(t - t_k),\ F_k := F(t_k),\ G_k := \frac{F(t_{k+1}) - F(t_k)}{\delta t}, \tag{63}$$

for $t \in [t_k, t_{k+1}]$ as $k = 0, \dots, N-1$. Then, a discrete solution e^N to (57) can be found by the numerical quadrature based on the formula (62) for $F = F^N$ from (63) under subsequent iterations $t \in [t_k, t_{k+1}]$ as $k = 0, \dots, N-1$:

$$e^N(t) = \frac{1}{\alpha_1}\left[F_k + G_k\left(t - t_k - \frac{\alpha_2}{\alpha_1}\right) + \left(\alpha_1 e^N(t_k) - F_k + G_k\frac{\alpha_2}{\alpha_1}\right)\exp\left(\frac{\alpha_1(t_k-t)}{\alpha_2}\right)\right]. \tag{64}$$

We note that it turns into (62) at $k = 0$ for $N = 1$.

We use the formulae (62)–(64) to carry out the numerical integration to present the result of our numerical tests under monotone and cyclic pressure loading.

4.1 | Monotone pressure loading

Let the pressure be prescribed by a linear function

$$p(t) = gt \text{ for } t \in [0, T], \tag{65}$$

with the constant gradient g. To outline admissible mechanical pressures, we remark that attaining the critical pressure $p_{\rm cr} := 1/(3b)$, the right-hand side of the reference response equation (57) becomes infinite, whereas this singularity is avoided within the thresholding (58) and the linearized equation (59).

For definiteness, we set the values of parameters for concrete from Murru et al. [36]: Young's modulus $E = 30$ (GPa) and Poisson's ratio $\nu = 0.2$ such that according to (16), the shear modulus $\alpha_1 = 25$ (GPa) and $a = 0.5$; the viscosity $\alpha_2 = 10$ (GPa·h), $b = 0.01$ (1/GPa) such that $p_{\rm cr} = 33.(3)$ (GPa), and the lower threshold $\underline{M} = 0.2$.

The pressure loading (65) is shown by the straight line versus time $t \in [0, 1.3]$ (h) in the plot (A) of Figure 1. The loading gradient $g = 33.(3)$ (GPa/h) is chosen such that in time $t = 1$ h, the critical pressure $p_{\rm cr}$ will be attained. The corresponding discrete solution e^N to the nonlinear equation (57) calculated with the time step $\delta t = 0.02$ is portrayed versus pressure $p \in [0, p_{\rm cr})$ in the plot (C) of Figure 1. We observe that approaching $p_{\rm cr}$, marked by the vertical dashed line, the solution e^N blows up to minus infinity. In marked contrast, analytic solution e to the linearized Kelvin–Voigt equation (59) continues after $p_{\rm cr} = 33.(3)$ as portrayed versus $p \in [0, 43.(3)]$ in the plot (B) of Figure 1.

To overcome the difficulty of blow-up, the thresholding solution to Equation (58) first follows the nonlinear equation (57) within $p \in \left[0, p_{\rm cr}\left(1 - \underline{M}\right)\right]$, where the denominator $1 - p/p_{\rm cr}$ is bounded by $\underline{M}$ from zero. After the threshold pressure $p_{\rm cr}\left(1 - \underline{M}\right) = 26.(6)$ (GPa), the solution switches to the linearized Kelvin–Voigt equation (59). The corresponding function $\mathcal{F}[-3p]$ is shown in the plot (B) of Figure 2 by the solid line in comparison with the pressure without thresholding presented here by the dashed line. The thresholding dilatation e versus $p \in [0, 43.(3)]$ is depicted by the solid line in the plot (C) of Figure 2.

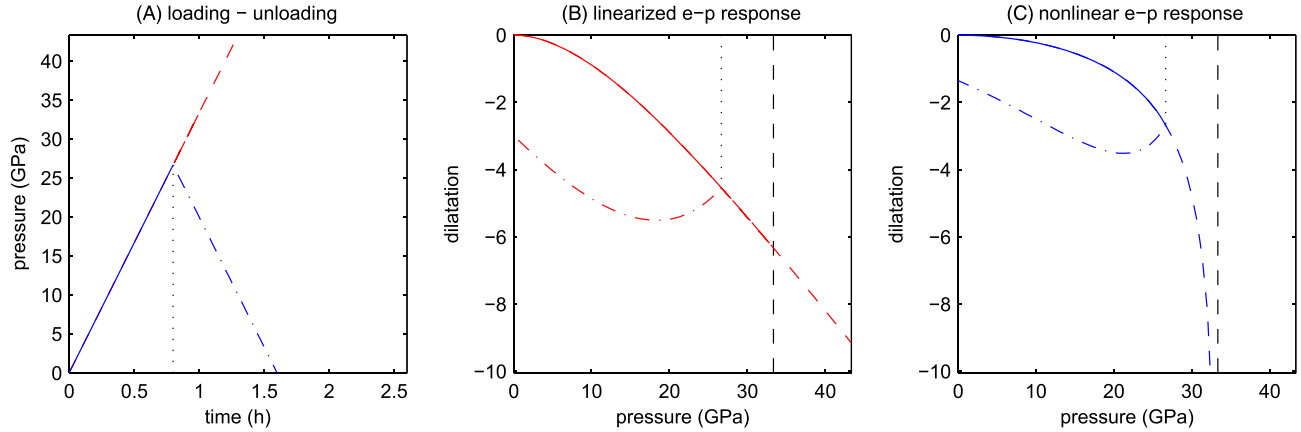

FIGURE 1 Corresponding to pressure $p(t)$ in plot (A), the corresponding response dilatation $e(p)$ in plot (B) for linearized model (59), and in plot (C) for nonlinear (57) viscoelastic model. [Colour figure can be viewed at wileyonlinelibrary.com]

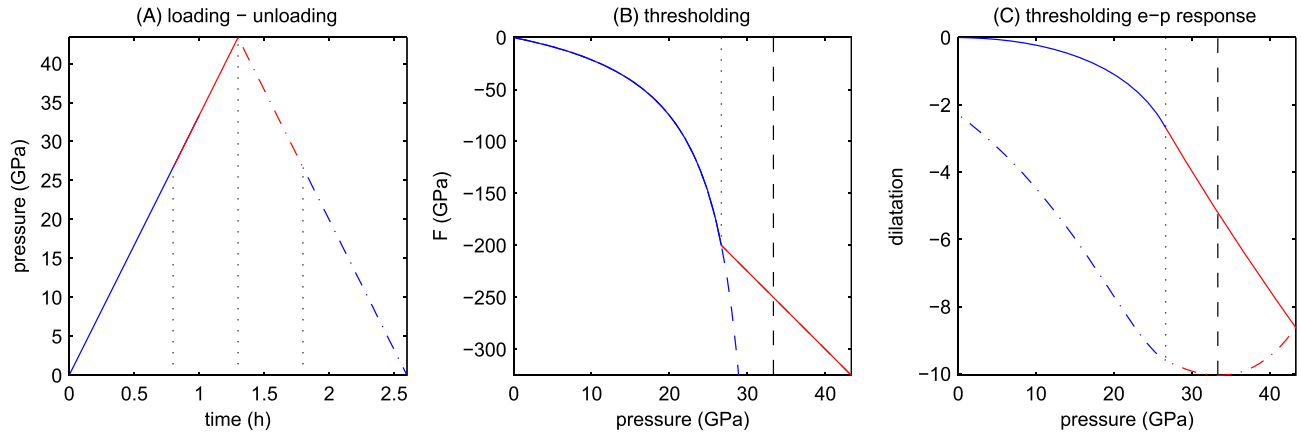

FIGURE 2 Corresponding to the pressure $p(t)$ in plot (A) and thresholding $\mathcal{F}[-3p]$ in plot (B) and the corresponding response dilatation $e(p)$ for thresholding viscoelastic model (58) in plot (C). [Colour figure can be viewed at wileyonlinelibrary.com]

4.2 | Cyclic pressure loading–unloading

Let the cyclic pressure be prescribed by a triangular function p with the constant gradient g as before:

$$p(t) = \begin{cases} gt & \text{for } t \in [0, T/2] \\ g(T-t) & \text{for } t \in [T/2, T] \end{cases}, \tag{66}$$

which implies loading in the first phase $t \in [0, T/2]$, then unloading during $t \in [T/2, T]$.

First, we choose the period of the cycle $T = 1.6$ (h) such that the switching at $T/2 = 0.8$ (h) occurs at the pressure $p = p_{\text{cr}}\left(1 - \underline{M}\right)$ before the blow-up as shown in the plot (A) of Figure 1. The corresponding solutions to the linearized Kelvin–Voigt equation (59) and nonlinear equation (57) are portrayed versus pressure, respectively, in the plots (B) and (C) of Figure 1. In the figures, the loading is marked by a solid line, whereas the unloading by a dash-dotted line. The both cyclic solutions present an open loop. For comparison, the continuation after the switching point $p_{\text{cr}}\left(1 - \underline{M}\right) = 26.(6)$ by the monotone loading from (59) is marked here by a dashed line.

For the thresholding equation (58), we can choose in (66) the pressure cycle of period $T = 2.6$ (h), when loading switches to unloading at $T/2 = 1.3$ (h) corresponding to $p = 43.(3)$ after the critical pressure, as shown in the plot (A) of Figure 2. The thresholding solution to (58) is presented by a looped path portrayed versus cyclic pressure in the plot (C) of Figure 2. Again, the loading here is marked by a solid line and unloading by a dash-dotted line. By unloading, the thresholding function $\mathcal{F}[-3p]$ in the plot (B) of Figure 2 follows the same path as by loading.

5 | CONCLUSION

The numerical simulation under cyclic pressure was carried out in order to compare the solutions for the nonlinear, linearized, and thresholding viscoelastic models. In all the cases that were tested, the pressure-controlled dilatation exhibits an open loop in the loading–unloading cycle.

The thresholding model exhibits more reasonable response than the nonlinear viscoelastic model, in the sense that in the latter model, the solution may blow up under finite pressure under monotonically increasing or decreasing load. The material moduli in a linearized Kelvin–Voigt model (or for that matter the nonlinear Kelvin–Voigt) are constant. However, we expect most porous materials like concrete, rock, porous metals, bone, and ceramics, to have pressure-dependent material moduli, which was the reason for our carrying out the study for the constitutive relation (7).

AUTHOR CONTRIBUTIONS

All authors contributed equally to this work.

ACKNOWLEDGEMENTS

The authors acknowledge the financial support by the University of Graz. H. Itou is partially supported by Grant-in-Aid for Scientific Research (C) (18K03380) of Japan Society for the Promotion of Science (JSPS). V. A. Kovtunenko thanks the Austrian Science Fund (FWF) for support. K. R. Rajagopal thanks the Office of Naval Research and the National Science Foundation for their support.

CONFLICT OF INTEREST STATEMENT

The authors declare no potential conflict of interests.

ORCID

Hiromichi Itou https://orcid.org/0000-0002-6224-8031
Victor A. Kovtunenko https://orcid.org/0000-0001-5664-2625
Kumbakonam R. Rajagopal https://orcid.org/0000-0002-4636-5131

REFERENCES

1. K. R. Rajagopal, *On implicit constitutive theories*, Appl. Math. **48** (2003), 279–319, DOI 10.1023/A:1026062615145.
2. V. Průša and K. R. Rajagopal, *On implicit constitutive relations for materials with fading memory*, J. Non-Newton. Fluid Mech. **181–182** (2012), 22–29, DOI 10.1016/j.jnnfm.2012.06.004.
3. K. R. Rajagopal, *An implicit constitutive relation for describing the small strain response of porous elastic solids whose material moduli are dependent on the density*, Math. Mech. Solids **26** (2021), 1138–1146, DOI 10.1177/10812865211021465.
4. K. R. Rajagopal and A. S. Wineman, *A note on viscoelastic bodies whose material properties depend on the density*, Math. Mech. Solids **26** (2021), 1726–1731, DOI 10.1177/10812865211004663.
5. H. Itou, V. A. Kovtunenko, and K. R. Rajagopal, *On an implicit model linear in both stress and strain to describe the response of porous solids*, J. Elasticity **144** (2021), 107–118, DOI 10.1007/s10659-021-09831-x.
6. H. Itou, V. A. Kovtunenko, and K. R. Rajagopal, *Investigation of implicit constitutive relations in which both the stress and strain appear linearly, adjacent to non-penetrating cracks*, Math. Mod. Meth. Appl. Sci. **32** (2022), no. 7, 1475–1492, DOI 10.1142/S0218202522500336.
7. W. Thomson, *On the elasticity and viscosity of metals*, Proc. Roy. Soc. London A **14** (1865), 289–297, DOI 10.1098/rspl.1865.0052.
8. W. Voigt, *Über innere Reibung fester Körper, insbesondere der Metalle*, Annalen der Physik **283** (1892), 671–693.
9. L. Boltzmann, *Zur Theorie der elastischen Nachwirkung*, Annalen der Physik **241** (1878), 430–432, DOI 10.1002/andp.18782411107.
10. A. E. Green and R. S. Rivlin, *The mechanics of non-linear materials with memory. Part I*, Arch. Rational Mech. Anal. **1** (1957), 1–21, DOI 10.1007/BF00297992.
11. A. E. Green and R. S. Rivlin, *The mechanics of non-linear materials with memory. Part III*, Arch. Rational Mech. Anal. **4** (1959), 387–404, DOI 10.1007/BF00281398.
12. A. E. Green, R. S. Rivlin, and A. J. M. Spencer, *The mechanics of non-linear materials with memory. Part II*, Arch. Rational Mech. Anal. **3** (1959), 82–90, DOI 10.1007/BF00284166.
13. F. J. Lockett, *Non-linear viscoelastic solids*, Academic Press, London, 1972.
14. A. Muliana, K. R. Rajagopal, D. Tscharnuter, and G. Pinter, *A nonlinear viscoelastic constitutive model for polymeric solids based on multiple natural configuration theory*, Int. J. Eng. Sci. **100-101** (2016), 95–110, DOI 10.1016/j.ijsolstr.2016.07.017.

15. K. R. Rajagopal and A. S. Srinivasa, *On a class of non-dissipative materials that are not hyperelastic*, Proc. Roy. Soc. London A **465** (2009), 493–500, DOI 10.1098/rspa.2008.0319.
16. M. Bulíček, J. Málek, and K. R. Rajagopal, *On Kelvin–Voigt model and its generalizations*, AIMS Evol. Eq. Control Theory **1** (2012), 17–42, DOI 10.3934/eect.2012.1.17.
17. M. Bulíček, V. Patel, Y. Şengül, and E. Süli, *Existence of large-data global weak solutions to a model of a strain-limiting viscoelastic body*, Commun. Pure Appl. Anal. **20** (2021), 1931–1960, DOI 10.3934/cpaa.2021053.
18. H. Itou, V. A. Kovtunenko, and K. R. Rajagopal, *On the states of stress and strain adjacent to a crack in a strain-limiting viscoelastic body*, Math. Mech. Solids **23** (2018), 433–444, DOI 10.1177/1081286517709517.
19. H. Itou, V. A. Kovtunenko, and K. R. Rajagopal, *On the crack problem within the context of implicitly constituted quasi-linear viscoelasticity*, Math. Mod. Meth. Appl. Sci. **29** (2019), no. 2, 355–372, DOI 10.1142/S0218202519500118.
20. H. Itou, V. A. Kovtunenko, and K. R. Rajagopal, *The Boussinesq flat-punch indentation problem within the context of linearized viscoelasticity*, Int. J. Eng. Sci. **151** (2020), 103272, DOI 10.1016/j.ijengsci.2020.103272.
21. H. Itou, V. A. Kovtunenko, and K. R. Rajagopal, *Lagrange multiplier approach to unilateral indentation problems: well-posedness and application to linearized viscoelasticity with non-invertible constitutive response*, Math. Mod. Meth. Appl. Sci. **31** (2021), no. 3, 649–674, DOI 10.1142/S0218202521500159.
22. H. Itou and A. Tani, *Existence of a weak solution in an infinite viscoelastic strip with a semi-infinite crack*, Math. Mod. Meth. Appl. Sci. **14** (2011), no. 7, 975–986, DOI 10.1142/S0218202504003519.
23. A. M. Khludnev, Contact viscoelastoplastic problem for a beam, *Problems in continuum mechanics*, S. N. Antontsev, K.-H. Hoffmann, and A. M. Khludnev, (eds.), Birkhäuser, Basel, 1992, pp. 159–166.
24. A. M. Khludnev and V. A. Kovtunenko, *Analysis of cracks in solids*, International Series on Advances in Fracture, Vol. **6**, WIT Press, Southampton, Boston, 2000.
25. V. A. Kovtunenko, *Numerical simulation of the non-linear crack problem with non-penetration*, Math. Meth. Appl. Sci. **27** (2004), no. 2, 163–179, DOI 10.1002/mma.449.
26. T. S. Popova, *Problems of thin inclusions in a two-dimensional viscoelastic body*, Int. J. Pavement Eng. **12** (2018), 313–324, DOI 10.1134/S1990478918020114.
27. K. R. Rajagopal, *Remarks on the notion of "pressure"*, Int. J. Nonlinear Mech. **71** (2015), 165–172, DOI 10.1016/j.ijnonlinmec.2014.11.031.
28. M. Bulíček, P. Gwiazda, J. Málek, K. R. Rajagopal, and A. Świerczewska-Gwiazda, On flows of fluids described by an implicit constitutive equation characterized by a maximal monotone graph, *Mathematical aspects of fluid mechanics*, J. Robinson, J. Rodrigo, and W. Sadowski, (eds.), Cambridge University Press, Cambridge, 2012, pp. 23–51.
29. M. Bulíček, J. Málek, and E. Süli, *Existence of global weak solutions to implicitly constituted kinetic models of incompressible homogeneous dilute polymers*, Commun. Part. Differ. Equ. **38** (2013), 882–924, DOI 10.1080/03605302.2012.742104.
30. F. E. Browder, *Nonlinear maximal monotone operators in Banach space*, Math. Annalen **175** (1968), 89–113, DOI 10.1007/BF01418765.
31. G. J. Minty, *Monotone (nonlinear) operators in hilbert space*, Duke Math. J. **29** (1962), 341–346, DOI 10.1215/S0012-7094-62-02933-2.
32. H. Itou, V. A. Kovtunenko, and E. M. Rudoy, *Three-field mixed formulation of elasticity model nonlinear in the mean normal stress for the problem of non-penetrating cracks in bodies*, Appl. Eng. Sci. **7** (2021), 100060, DOI 10.1016/j.apples.2021.100060.
33. V. A. Kovtunenko, *A hemivariational inequality in crack problems*, Optimization **60** (2011), no. 8-9, 1071–1089, DOI 10.1080/02331934.2010.534477.
34. M. Sofonea and S. Migórski, *Variational–hemivariational inequalities with applications*, Chapman and Hall/CRC, Boca Raton, 2017.
35. W. Noll, *A new mathematical theory of simple materials*, Int. J. Pavement Eng. **48** (1972), 1–50, DOI 10.1007/BF00253367.
36. P. T. Murru, C. Torrence, Z. Grasley, K. R. Rajagopal, P. Alagappan, and E. Garboczi, *Density-driven damage mechanics (D3-M) model for concrete I: mechanical damage*, Int. J. Pavement Eng. **23** (2022), no. 4, 1161–1174, DOI 10.1080/10298436.2020.1793983.

How to cite this article: H. Itou, V. A. Kovtunenko, and K. R. Rajagopal, *A generalization of the Kelvin–Voigt model with pressure-dependent moduli in which both stress and strain appear linearly*, Math. Meth. Appl. Sci. **46** (2023), 15641–15654. DOI 10.1002/mma.9417